CHAPTER - V I

CHAPTER-VI

DC ELECTRICAL RESISTIVITY STUDY OF GRANULARITY IN BULK $YBa_2Cu_3O_7$/Ag COMPOSITES

VI.1 Introduction

With an aim to understand the charge transfer mechanism in a granular medium like the bulk $YBa_2Cu_3O_{7-y}$(YBCO) sinters, the present chapter analyzes the temperature dependence of resistivity in a set of YBCO/Ag composites where granularity control is effected by varying the Ag volume fraction. A percolative charge conduction model allows us to extract the parameters from the $\rho(T)$ characteristics which quantify granularity and whose variation with Ag content indicates the microstructural modifications brought about by Ag in the composites. The result points to a mechanism of grain growth in the composites which accounts for the narrower grain size distribution in these systems as compared to that in Ag free YBCO sinters.

VI.2. Experimental

The preparation procedure of the YBCO phase that was used as the precursor along with Ag_2O for the composites is detailed in chapter III. The superconducting samples of YBCO/Ag composites with varying Ag volume fraction from 0 to 54 vol.% were prepared. The samples were cold pressed into pellets, annealed at 930 C for 12 hrs and cooled to 500 C where they stayed for 12 hrs with oxygen flowing. The samples were then cooled to room temperature (RT) at a rate 2 C/min and cut into rectangular shapes for DC four probe resistivity measurements.

The measuring current density, j was 30 mA/cm^2. Percolative lengthening of current paths in granular medium like that in our samples, is expected to make the effective current density, j_e in them different from j. For each sample, j_e as estimated from the expression $j_e = j/\alpha$ (where α is the current percolation factor as discussed later) was found to vary from 150 mA/cm^2 in samples with lowest granularity to 300 mA/cm^2 in samples with highest granularity. These currents were found to be well below the values for which the Tc and ΔTc showed a current dependence. For temperature dependent resistivity measurement, the samples were cooled to 10 K by the closed cycle He refrigerator and the ρ vs T data were taken by a computer controlled data acquisition system during heating of the sample to RT. The heating rate was confined to 3 K per minute.

VI.3. Results and Discussion

VI.3.1. Ag induced modification of electrical transport in YBCO/Ag composites

The temperature dependence of the electrical resistivity of YBCO and YBCO/Ag composites with Ag vol.% of 0, 5.9, 19.5 and 54 is shown in Fig. VI.1. In agreement with several authors [1-3], a decrease in normal state resistivity of the composites with increasing Ag volume fraction with Tc remaining constant up to the highest Ag volume fraction (54%) was observed. For all the samples, the normal state resistivity increases linearly with temperature beyond the superconducting order parameter fluctuation (SCOPF) region. Linear fitting of the ρ vs T data in a typical temperature interval from 150 to 250 K, thus avoiding the SCOPF region, yielded the resistivity slope $d\rho/dT$ and the residual resistivity ρ_0 (normal state resistivity extrapolated to T= 0 K as shown in Fig. VI.1) for different Ag composites. Both these parameters contain information on granularity [4-8] and show dramatic decrease with increasing Ag vol% (Table VI.1).

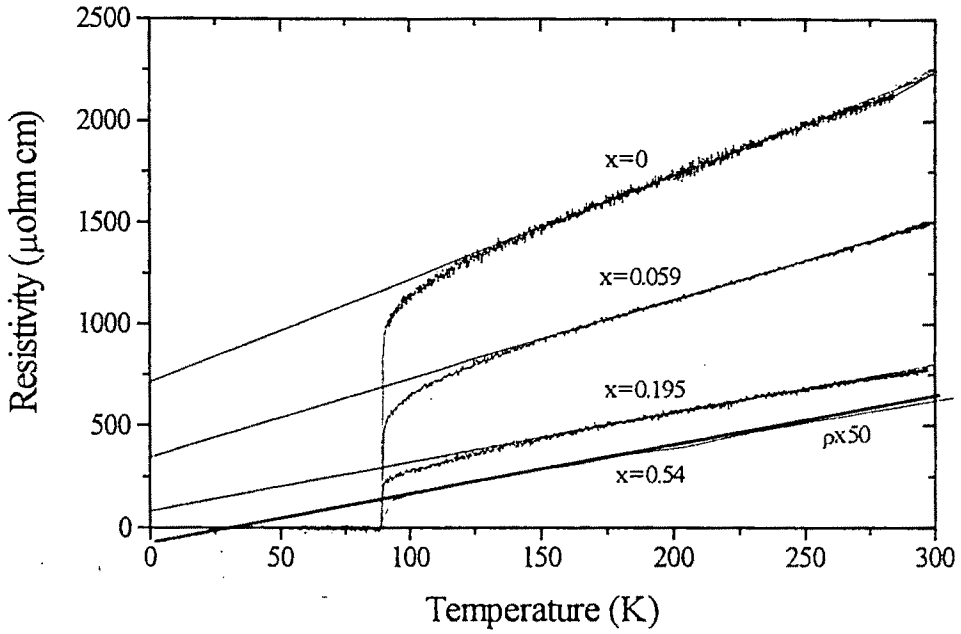

Fig. VI.1. Temperature dependence of the resistivity of YBCO/Ag (x vol.%) composites. Linear fitting of the resistivity in the temperature range 150 to 250 K and extrapolated to 0 K gives resistivity slope ($d\rho/dT$) and residual resistivity (ρ_0).

Table VI.1. Variation of the parameters quantifying granularity in the composites with Ag vol%.

Ag vol.%	ρ_{300K}/ρ_{100K}	$1/\rho(d\rho/dT)$ $(10^{-3}K^{-1})$	$d\rho/dT$ (μ ohm cm K^{-1})	ρ_0 (μ ohm cm)	ρ_{wl} (μ ohm cm)	α
0	2.0	2.26	5.08	714.1	70.31	0.098
5.9	2.3	2.58	3.87	346.3	44.74	0.129
19.5	2.74	3.13	2.40	83.54	17.37	0.208
54	3.53	3.59	0.046	-1.28	-	-

According to Matthiessen's rule, ρ_0, which results from temperature-dependent impurity scattering, should not be related to the electron-phonon interaction yielding $\rho(T)$ or the slope $d\rho/dT$. The apparent deviation from Matthiessen's rule as observed in our case with $d\rho/dT$ scaling with ρ_0 in different composites (Table VI.1) is in agreement with Lin et al. [9] and arises due to percolative lengthening of current paths in granular medium in general and in sintered HTSC systems with randomly oriented anisotropic grains in particular [4] as discussed latter.

The magnitude of ρ_0 which is a measure of the grain boundary resistivity [9-11] decreases at a much faster rate as compared to ρ_{300K} with increasing Ag volume fraction within the percolation threshold for conduction through Ag channels (~20 vol.%) [9]. This can be seen by comparing their normalized values (Fig. VI.2). While ρ_0 remained positive for samples with Ag volume fraction increasing from 0 to 19.5 vol.%, it showed a negative value for 54 vol.% (Table VI.1). The negative intercept of resistivity at T = 0 K for Ag volume fraction beyond its percolation threshold is like the Bloch Gruneisen behaviour typical for metals [12]. This type of behaviour can be understood as arising due to highly conducting Ag channels dominating the percolative conduction in the composites [9]. Within the percolation limit however, Ag brings about considerable modifications in the grain boundary characteristics.

In the frame work of the percolative conduction model of Halbritter et al. [10], the temperature dependence of the resistivity of granular YBCO can be expressed as

$$\rho(T) = \rho_B + P\,(\rho_0^{\,i} + \alpha^i T) \qquad (1)$$

Here $\rho_0^{\,i} + \alpha^i T$ is the intrinsic resistivity of the grains ($\alpha^i = d\rho_i/dT$). P (≥ 1) is an effective-area factor which takes into account the percolative nature of the conducting paths. ρ_B is the temperature-independent residual resistivity of the grain boundaries. For single crystals and epitaxial thin films, both ρ_B and $\rho_0^{\,i}$ have negligible contribution to the total resistivity, and P = 1. Eqn. VI.1 in these cases therefore leads to

$$1/\rho(d\rho/dT) \sim 1/T \qquad (2)$$

and with a constant $d\rho/dT$

$$\rho_{300K} / \rho_{100K} = 3 \qquad (3)$$

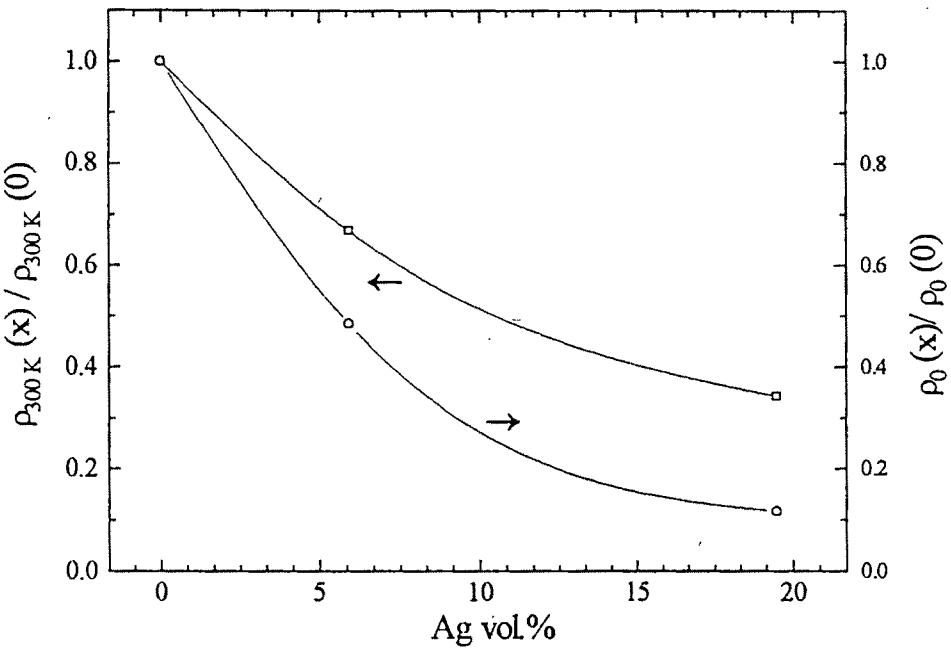

Fig. VI.2. The variation of normalized room temperature resistivity $\rho_{300K}(x)/\rho_{300K}(0)$ (squares) and normalized residual resistivity $\rho_0(x)/\rho_0(0)$ (circles) with Ag volume fraction, x.

Our observation of ρ_{300K}/ρ_{100K} increasing from 2 (Table VI.1) in granular YBCO samples to 2.3 in samples with 5.9 vol.% of Ag and further to 2.74 for 19.5 vol.% Ag clearly shows that it approaches the intrinsic value of 3 with Ag vol.% approaching the percolation threshold. Above the percolation threshold, ρ_{300K}/ρ_{100K} increases to a large value of 3.53 in our 54 vol.% of Ag sample in agreement with Lin et al. [9] and arises due to conduction prevalently through Ag channels. The resistivity behaviour of the composites approaching to that of the single crystals and epitaxial films with increasing Ag concentration within the percolation threshold is also evidenced from the variation of the temperature coefficient of resistivity, $1/\rho(d\rho/dT)$ measured at 300 K with Ag vol.% which shows a rather sharp increase from 2.26 $x10^{-3}$ K^{-1} in the highly granular Ag free YBCO to 3.13 x 10^{-3} K^{-1} in the composite with 19.5 vol.% Ag (Fig. VI.3), thus approaching the intrinsic value of 3.3 x 10^{-3} K^{-1} [9] as the Ag content approaches the percolation threshold.

The strong dependence of the resistivity slope $d\rho/dT$ on the preparation conditions of different polycrystalline YBCO (Ag free) sinters as observed by Halbritter et al. [10] directly correlates with that of our composite samples prepared under the same condition but with different Ag vol.%. Assuming the intragrain (ab-plane) resistivity to be identical for different batches of samples, Diaz et al. [11] have shown that the measured resistivity can vary from one batch of YBCO sinters to another batch depending on the variation in their intergranular resistivity.

To estimate the extent of granularity in sintered YBCO samples, $d\rho/dT$ vs ρ_{100k} (resistivity at a temperature close to Tc) has often been used in the literature [4,9]. In Fig. VI.4 we present the $d\rho/dT$ vs ρ_{100k} data (star symbol) for our YBCO/Ag composites with different Ag vol.% (mentioned in the parenthesis). Also included in this figure is a straight boarder line constructed with $d\rho/dT$ data for single crystals [13] and epitaxial thin films [14] of YBCO with varying oxygen content [9,10]. Experimentally it has been found that

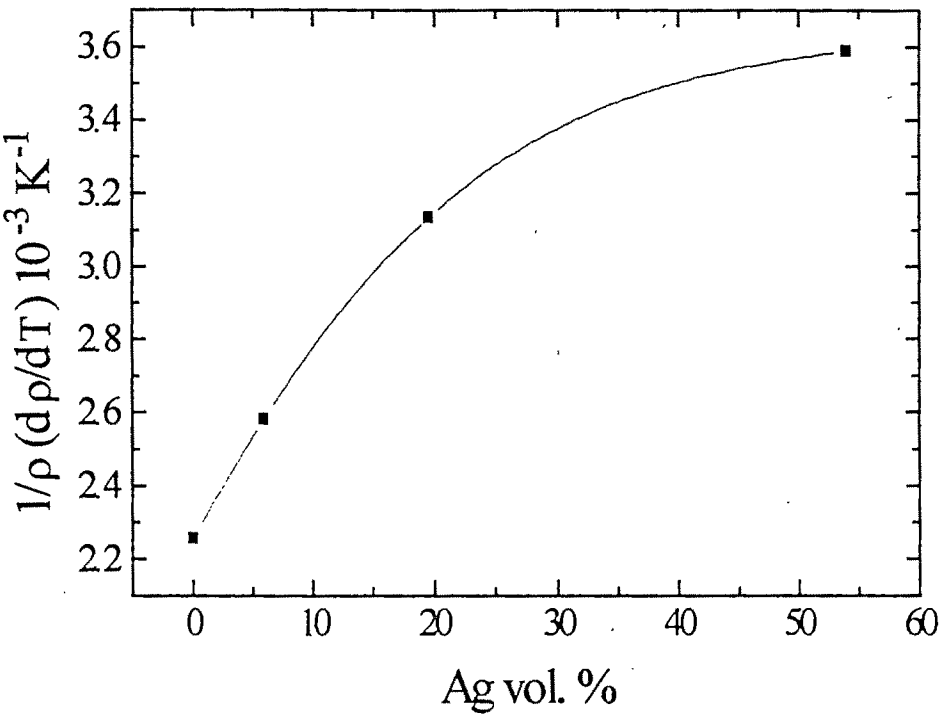

Fig.VI.3. The variation of temperature co-efficient of resistivity $1/\rho(d\rho/dT)$ with Ag volume fraction.

dρ/dT for polycrystalline YBCO samples lies on the top or on the right side of this line depending on the granularity of the samples [9]. More granular a sample is, dρ/dT deviates more to the right of the line. This is evidenced from dρ/dT data of Ag free YBCO samples with varying granularity taken from [9] and plotted as a dotted line in Fig. VI.4. The dρ/dT of our composite samples with varying Ag vol.% falling almost on this dotted line and approaching the boarder line at higher Ag vol.% clearly shows the dramatic effect of Ag in controlling granularity in sintered cuprates. At Ag vol.% just beyond the percolation threshold, it is interesting to note that ρ_{100k} approaches the intrinsic value of 50 μ ohm.cm which is the value corresponding to ρ_{ab} measured in single crystals.

Suppression of granularity in the composites with increasing Ag content is also evidenced from the almost linear dependence of ρ_0 on ρ_{100K} of the composites with varying Ag vol.% (Fig. VI.5). The ρ_0 has the contribution of both the grain boundary resistivity and resistivity due to flaws and defects inside the grains. On extrapolation, ρ_0 goes to zero at $\rho_{100\,k}$ = 177 μohm. cm. This is in agreement with observation of Lin et al. [9] that in general dρ/dT of polycrystalline samples lies on the boarder line only when ρ_{100K} is less than 200 μohm. cm. In this state, the system response tends to be that of single crystals and epitaxial thin films with $\rho_0 = 0$. A comparison of our observations on YBCO/Ag composites with the observations made by many authors [9,10] on Ag free YBCO imply that while granularity in sintered YBCO is controlled by controlling preparation conditions, granularity in YBCO/Ag composite samples, all prepared under identical conditions, seems to be controlled by Ag vol.%.

VI.3.2. Current conduction below and above Ag percolation threshold

In YBCO/Ag composites with Ag concentration between 20 to 70 vol.%, percolative networks of both YBCO and Ag exist [9,15]. Current

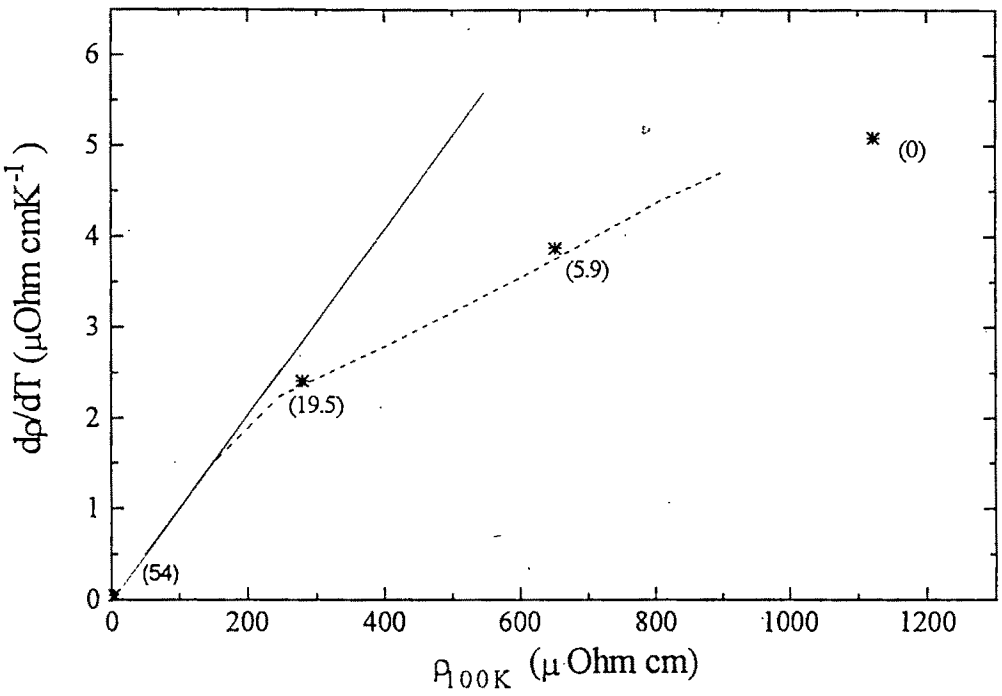

Fig.VI.4. The variation of resistivity slope (dρ/dT) with ρ_{100K} for different Ag composites (star symbol). The number in the parentheses indicates the Ag volume fraction. The dashed line corresponds to the (dρ/dT) of granular Ag free YBCO samples with varying granularity [9]. The straight boarder line passing through the origin gives the (dρ/dT) of single crystals and epitaxial thin film as discussed in the text.

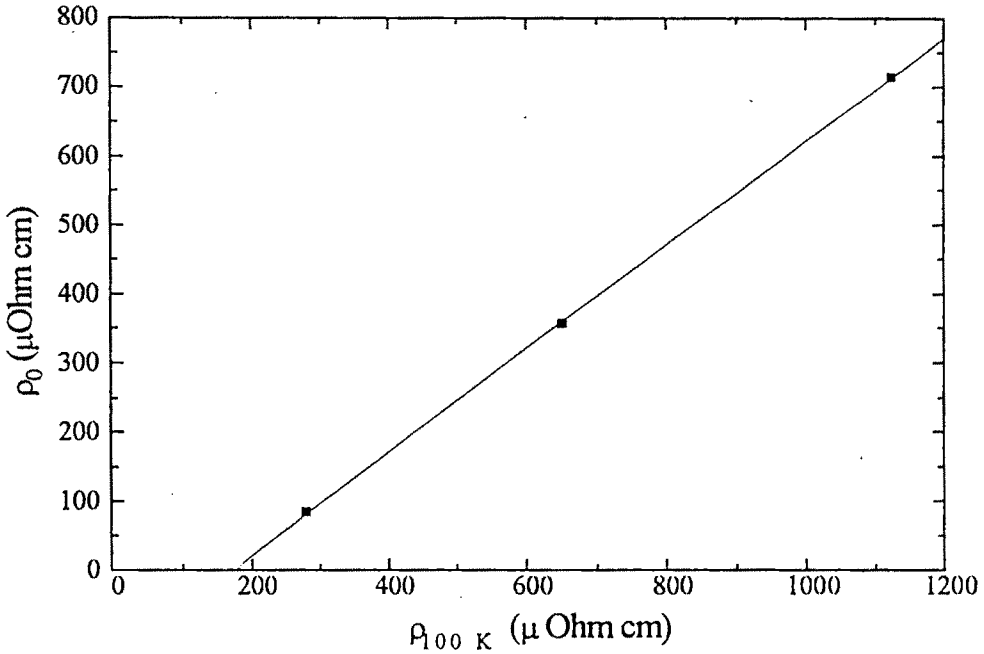

Fig.IV.5. The variation of residual resistivity ρ_0 with ρ_{100K} for different Ag composites. The extrapolation of the line shows that ρ_0 goes to zero for ρ_{100K} = 177 μohm cm which is the ρ_{100K} value on the boarder line where deviation due to granularity begins as shown in figure 4.

conduction in such a system has been analyzed in a two resistance model [1] which speculate that in the normal state, the current prevalently passes through the highly conducting Ag channels and below Tc, the supercurrent percolates through the YBCO grains. The reduction in the normal state resistivity by two orders of magnitude in the composite with 54 vol.% of Ag as compared to that in Ag free YBCO with Tc almost remaining unchanged (Fig. VI.1) is in accordance with the two resistance model and is in agreement with the observations made by many [2,16,17]. For Ag concentration below 20 vol.% i.e. below the Ag percolation threshold however, the current is mostly carried through the percolating YBCO grains both above and below Tc. In this concentration regime of Ag, it is expected that the resistivity in the normal state and its temperature coefficient should not vary much from that of Ag free YBCO. The resistivity data (Fig. VI.1) however shows that for Ag vol.% of 19.5 which is just below the Ag percolation threshold, resistivity at 300 K decreases by a factor of 3 while for 5.9 vol.% which is much lower than the percolation threshold, this decrease is by a factor of 1.5 from that of the Ag free YBCO. Jung et al. [18] have obtained similar trend in resistivity decrease with increasing Ag volume fraction within the percolation limit. On the other hand, with the same Ag volume fraction many authors have obtained still higher resistivity decrease [8,9,19]. This discrepancy in the magnitude of resistivity decrease on Ag volume fraction as observed by different authors may arise due to the sample preparation conditions. Nevertheless, the large decrease in the resistivity observed by us and by many other authors clearly indicates that the simple percolation model is inadequate to explain the current conduction process in the composites for Ag vol.% below the percolation threshold. In fact, presence of Ag brings about a significant modification in the microstructure of the composites. To understand the effect of microstructural modification on the normal state resistivity, we analyze below the temperature dependent resistivity data of YBCO/Ag composites based on a percolative current conduction model proposed by Diaz et al. [6].

VI.3.3. Percolative current conduction model for estimation of granularity parameters in YBCO/Ag composites

Studying the temperature variation of resistivity and critical current in samples of varying granularity, Diaz et al. [8,11] showed that current conduction process through grains and grain boundaries of sintered YBCO pellets is significantly modified by path lengthening factors arising due to misalignment of highly anisotropic grains and structural defects like voids and cracks. The observed normal state resistivity thus takes the form [6]

$$\rho = 1/\alpha[\rho_{ab}+\rho_{wl}] \qquad (4)$$

where ρ_{ab} is the intragrain resistivity in the ab-plane which has the same value as measured in single crystals. ρ_{wl} is the average weak link resistivity across the grain boundaries. The factor $\alpha = f \,.\, \alpha_{str}$ contains contribution of both the path lengthening factors f arising due to blocking of current across the misaligned surface of the highly anisotropic grains and α_{str} due to voids and microcracks. These parameters induce percolative conduction of transport current in the granular cuprates. Depending on the degree of texurization and the sample dependent defects, the factors f and α_{str} take the values between 0 and 1. Because of the extreme anisotropy of copper oxides, the in-plane resistivity ρ_{ab} is orders of magnitude less than that of out-of-plane resistivity ρ_c. Thus, ρ_c does not appear in eqn. VI.4. Instead, it is assumed that total current blockage along pathways with misaligned grains occur which induces current frustration and contributes to the grain misalignment factor f. ρ_{ab} being the intragranular resistivity, granularity in sintered YBCO is essentially characterized by α and ρ_{wl}.

The Tc_{on} represents the onset of superconductivity in the grains of the YBCO/Ag composites. It remains unaffected by the presence of Ag up to 54 vol.% as observed in the present study and up to even higher than the

superconducting percolation limit i.e. 70 vol.% of Ag as observed by other authors [9]. This indicates that Ag does not affect intragrain properties. The almost non-reactivity of Ag with YBCO is also confirmed from XRD studies [20]. Therefore, the intragrain resistivity ρ_{ab} in eqn. VI.4 is not expected to be modified in the composites. As discussed later in this section, the weak link resistivity ρ_{wl} and the path lengthening factor α however are affected much.

As seen in Fig. VI.1, the normal state resistivities of all the samples are linear in temperature. Following the procedure of Diaz et al. [6] this linearity of ρ allows us to calculate the parameters ρ_{wl} and α for different Ag volume fractions in the composites as shown below. ρ_{wl} is assumed to be independent of temperature above Tc. The α_{str} is thus obtained from the temperature derivative of eqn. VI.4 as

$$d\rho/dT = (1/\alpha)(d\rho_{ab}/dT) \qquad (5)$$

From eqn. VI.4 and VI.5 and assuming the intragranular resistivity ρ_{ab} to have a negligible intercept at 0 K, ρ_{wl} is determined as

$$\rho_0 = (1/\alpha)\,\rho_{wl} \qquad (6)$$

In single crystals and epitaxial thin films, α can take a value close to 1. In sintered bulk samples, depending on the extent of granularity, α gets reduced and approaches zero at percolation limit where current conduction is completely blocked. In the above analysis, the weal link resistivity ρ_{wl} is assumed to be temperature independent above Tc and ρ_{ab} is assumed, based on single crystal measurement [12], to vary linearly with temperature ($d\rho_{ab}/dT = 0.5\ \mu$ ohm cm K^{-1}) with a negligible intercept.

Though normal state resistivity and its temperature dependence are influenced to a large extent by Ag vol.%, the intrinsic ab-plane resistivity of the grains or its temperature dependence, as shown later remains unaffected and corresponds to that of undoped single crystals. The change in the measured resistivity slope $d\rho/dT$ in the composites therefore directly gives the value of α and its dependence on Ag vol.%. The weak link resistivities ρ_{wl} for different Ag vol.% are obtained from the corresponding residual resistivity ρ_0 and α. The values of ρ_{wl} and α thus obtained for the composites with different Ag vol.% are given in Table VI.1. It should be noted that the magnitude of ρ_{wl} represents the average weak link resistivity in a granular medium and is the physically relevant resistivity of polycrystalline materials for comparison with models and theories of junctions, weak link structure etc.

The individual junctions may have their characteristic weak link resistance depending on the nature of the junction and the strength of the coupling between the grains. The finite tailing at the low temperature side of the superconducting transition is in fact a consequence of the distribution in the magnitude of ρ_{wl}'s. The nature of distribution, whether Gaussian or otherwise, can be ascertained from a detailed analysis of the current-voltage characteristics in a temperature range in the superconducting state close to the Tc_0. The situation is similar to that of Tc inhomogeneity arising due to intragranular defects that influence the excess conductivity in the SCOPF regime [7]. Analysis of the distribution of ρ_{wl} however, is not attempted here. Neither have we attempted to find out the effect of highly resistive grain boundaries occurring on the tail end of the ρ_{wl} distribution on blocking the current paths and contributing to percolative effect. We just note here that in the applicability of eqn. VI.4, approximation in regards to weak link conductivity and percolative effects are made by neglecting the above effects. These approximations, however have been successfully used in a variety of situations such as fluctuation-induced conductivity in small metal particles, dc

conductivity, paraconductivity, critical currents in granular copper oxides, etc [5, 8].

To test the applicability of the approximations to the present case, we have scaled the $\rho(T)$ of the composites with varying Ag vol.% with their α and ρ_{wl} values and plotted the temperature dependence of $\alpha.\ \rho(T)- \rho_{wl}$ in Fig. VI.6, as has been done by Diaz et al. [8] for $Bi_{1.5}Pb_{0.5}Sr_2Cu_3O_y$ samples of varying granularity. In agreement with eqn. VI.4, $(\rho_{ab}(T) = \alpha.\ \rho(T) - \rho_{wl})$, Fig. VI.6 shows the intrinsic or sample independent nature of the plots corresponding to all the Ag vol.% studied. The almost coincidence of all the plots within experimental error, even inside the SCOPF region and matching with the ρ_{ab} vs T behavior of single crystals [21] indicate that Ag primarily resides at the grain boundary, modifies the intergranular behaviour and current percolation, and does not affect the intragranular properties [2,18].

VI.3.4. Evolution of Granularity Parameters with Ag Concentration

To analyze the current percolation process in the composites, we now compare the magnitudes of their inter- and intragranular resistivities. ρ_{wl} in our Ag free YBCO samples is 70 μohm. cm (Table VI.1). This value is of the same order as $\rho_{ab}(T)$, which varies from 50 μohm. cm at 100 K to 150 μohm. cm at 300 K (Fig. VI.6). Increasing Ag volume fraction to 54%, which is well above the Ag percolation threshold (~ 20 vol.%), the residual resistivity ρ_0 shows a negative value. As discussed earlier, this is a consequence of the Bloch Grueneisen behaviour typical of metals. Within the percolation threshold, however, Ag brings about considerable microstructural modifications in the grain boundary characteristics that make the weak link resistivity ρ_{wl} fall below the intragranular resistivity ρ_{ab} (Table VI.1) and approach to zero with increasing Ag vol.%. ρ_{wl} being of the same order or even less than ρ_{ab} at higher Ag concentration clearly indicates that ρ_{wl} does not block the current paths. Current frustration arises solely due to misaligned grains and sample defects such as voids and microcracks leading to

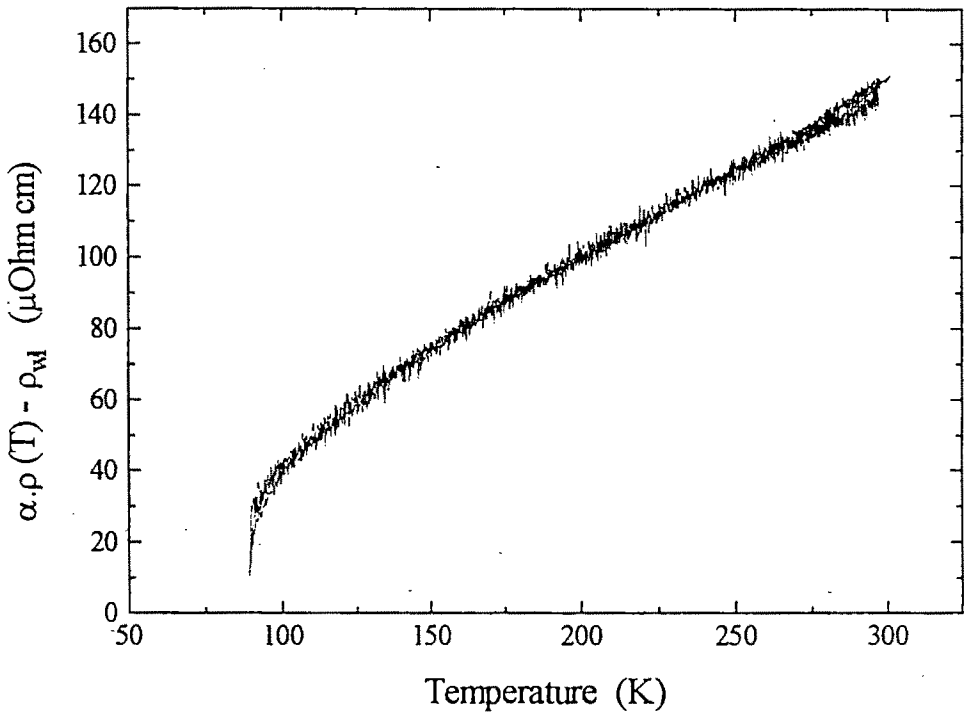

Fig.VI.6. Intragranular resistivity vs temperature curves obtained by scaling the $\rho(T)$ of the composites with varying Ag vol.% with their α and ρ_{wl} values as $\rho_{ab}(T) = \alpha.\rho(T) - \rho_{wl}$ where α and ρ_{wl} are the granularity parameters of the sample.

percolation factor α as discussed earlier. The factors ρ_{ab} and ρ_{wl} are scaled to the same extent to give the measured resistivity in our sintered composites (eqn. VI.4). The interdependency of $d\rho/dT$ and ρ_0 is therefore a simple consequence of these parameters being influenced by the same percolative factor α (eqn. VI.4 and 5) and explains the apparent deviation from Matthissen's rule.

From the above analysis it is clear that identification of the two parameters α and ρ_{wl} in the granular medium of the composite samples and their variation with Ag concentration gives a better understanding of the influence of Ag in bringing about the microstructural modification than a comparison of just the magnitude of normal state resistivity or even the magnitude of ρ_0 and $d\rho/dT$ as has been done by many [9,18]. The decrease of ρ_{wl} and increase of α at higher Ag vol.% (Table VI.1) indicates that the intergranular contribution to the total resistivity decreases and the resistivity response of the composites tends to be similar to that of single crystals and epitaxial thin films.

We now analyze the nature of $d\rho/dT$ variation with ρ_{100k} in sintered cuprates as shown in Fig. VI.4 in terms of the percolation model by Diaz et al. [6]. The $d\rho/dT$ on the y-axis is nothing but $d\rho_{ab}/dT$ scaled by the percolation factor α (eqn. VI.5). The ρ_{100k} shown on the x-axis can be expressed in terms of ρ_{ab} (100 K) and ρ_{wl}, once again scaled by the percolation factor α (eqn. VI.4). With $\rho_{ab}(T)$ and $d\rho_{ab}/dT$ corresponding to single crystal values, Fig. VI.4 represents the variation of α and ρ_{wl} for sintered YBCO with varying granularity (dotted line) or for the YBCO/Ag composites with varying Ag vol.% (star symbol). The magnitude of α and ρ_{wl}, thus quantifying the extent of granularity in different samples, determines the position of their x, y coordinates in Fig. VI.4.

Increasing Ag vol.% within its percolation threshold, ρ_{wl} decreases by a factor of 4 whereas $1/\alpha$ decreases by a factor of 2 (Table VI.1). Together, they contribute a decrease in ρ_0 by a factor of 8 as observed. The large decrease of

ρ_{wl} with increasing Ag vol.% is to be expected due to the following: First, Ag occupies the grain boundary regions of the composites. With its conductivity 3 orders of magnitude higher than that of YBCO, it will have a direct influence on the grain boundary resistivity, making it more metallic as compared to that of Ag free YBCO. Second, Ag dissolves the insulating phases such as $BaCuO_2$ and $BaCO_3$ occurring at the surface of the YBCO grains during sintering and clean the grain surfaces [20]. Both the factors can contribute to the decrease in ρ_{wl} with increasing Ag vol.% as observed.

The percolation factor α has the contribution of both the misalignment factor f and structural factor α_{str}. Since the misalignment effect is a consequence of the anisotropy in resistivity, the magnitude of f is expected to crucially depend on the aspect ratio of the grains. Assuming an ellipsoidal geometry for the YBCO grains, effective medium theory predicts the value of f as 1/3 in a randomly oriented YBCO system without pores, microcracks and other phases [6]. In YBCO/Ag composites, though global randomness may still be present, local alignment in the scale of grain dimension is to be expected due to grain surface melting and rearrangement of grains at the sintering temperature. Such type of grain alignment has been seen in thick films of YBCO/Ag composite sintered at a temperature higher than the peritectic temperature of YBCO [22] and leads to grain growth as discussed later. Since Ag is known to fill pores and microcracks and decreases porosity in the composites [2] α_{str} which is a measure of these structural defects, is expected to be strongly influenced by Ag volume fraction. The effect of Ag addition on both f and α_{str} causes an effective increase in α by 2 times at 19.5 vol.% of Ag, which is just below the percolation threshold.

Our observation of increase of α and decrease ρ_{wl} in composites prepared under identical conditions but with increasing Ag volume fraction correlates well with the variation of these parameters in pure YBCO samples prepared under different conditions [6]. This correlation clearly establishes

that granularity in sintered YBCO can be controlled by Ag addition as much as it can be controlled by preparation conditions.

VI.3.5. Improved grain growth behaviour

Though several speculations like grain surface melting [23] and grain surface cleaning [20,24] have been made in the literature to account for the observed grain growth behaviour, the mechanism of grain growth under Ag addition is still not clear. Not only Ag induces an increase in the grain size of YBCO by two to three times [18,20], it also significantly narrows down the grain size distribution. This latter aspect cannot be explained by the existing grain growth models.

As discussed above, the decrease of weak link resistivity ρ_{wl} and the increase of percolative factor α with increasing Ag volume fraction point mainly to two important directions i.e grains might be well connected and grain size might increase decreasing the length of the conducting path and increasing the area of cross section for percolative conduction. While the former aspect suggests the grain boundary becoming highly conducting due to Ag coating the YBCO grains as discussed above, the latter process suggests the enhanced grain growth on Ag addition. It has been shown by Ting and Lin [25] that the driving force for sintering is not only the reduction of surface energy i.e shrinkage of pores but also the reduction of grain-boundary energy i.e elimination of grain boundaries through grain growth. While the former is reflected in the increase of structural parameter α_{str} the later is a consequence of grain alignment and is reflected in misalignment factor f. Both these aspects contributing to the path lengthening factor α, increase with Ag volume fraction in the composites and lead to enhanced grain growth in the system. As Ag decreases the porosity of the composite system by a factor of half than Ag free YBCO [19], it facilitates migration of grain boundaries and grain growth begins [26]. The grain alignment induced by Ag in the composites

however has a distinct influence on the grain growth behaviour and the occurrence of uniform grain size in YBCO/Ag composites as discussed below.

At high annealing temperatures, the composite system has a large entropy and is driven to a highly metastable state. Self-organisation of the system involves many nonlinear mechanisms with positive feedback leading to dissipative structure formation. One of the processes of entropy stabilization and transition to a new state is the inter-particle diffusion of constituent ions across small angle grain boundaries which leads to grain growth. It has been shown by De et al. [20] and Deslande et al. [24] that Ag reacting with barium based compound such as $BaCuO_2$, $BaCO_3$ at the grain surface, clears the surface of the YBCO grains and causes partial melting at the grain boundary. With the availability of such a liquid phase at the grain boundary, YBCO grains in the composites become more mobile at the high annealing temperature and their entropy increases. The amplitude of the librational motion that the grains can execute is inversely proportional to the mass and size of the grains. Therefore, prior to the process of grain growth, the randomly oriented small size YBCO grains are expected to execute large amplitude librational motion. It should be noted here that unless the equivalent crystallographic planes of the anisotropic grains match at the boundary, inter-particle diffusion cannot occur. Hence fusion of two adjacent grains leading to grain growth will be inhibited. With increasing librational motion, the probability of crystallographic planes of two adjacent grains aligning with each other increases. At high annealing temperature, the liquid phase that Ag provides at the grain boundaries increases this probability and leads to the fusion of grains causing grain growth. Along with the growth of YBCO grains, the Ag also tend to cluster due to its higher cohesive force as compared to its adhesive force with YBCO [17]. This further enhances the kinetics of YBCO grains aiding in grain growth. During sintering, the silver attains its peritectic decomposition temperature forming a liquidous state. Silver has the characteristics of nonreactivity and catalytic effect on YBCO [27]. The

wetting properties of Ag reduces the surface tension [28] between the adjoining grains and enhances grain growth.

To understand the uniform grain size distribution in the composites, we analyze the process of entropy stabilization resulting out of the above grain growth behaviour. The inter-particle diffusion which initiates bonding between nearby grains, acts like an attractor in the process of non-equilibrium phase transition involving grain growth [29]. With increase in size of the grains, the kinetics of the grains is reduced and the associated entropy stabilization reduces the probability of further matching of the nearby grain surfaces. Such a process results into a restricted grain growth with restriction imposed by the optimum size reached beyond which kinetics is reduced for further growth. This leads to a nearly uniform grain size distribution in YBCO/Ag composites as against a large grain size distribution with smaller grains in Ag free YBCO.

VI.4. Conclusion

Analysis of the temperature dependence of normal state resistivity in a series of YBCO/Ag composites has enabled us to quantify the extent of granularity in these systems in terms of weak link resistivity across the grain boundaries and the current percolation factor arising from misaligned grains and sample dependent defects such as voids and cracks. Variation of these parameters with Ag vol.% indicates that contribution of granularity to the normal state resistivity decreases with increasing Ag vol.%. Thus, close to the Ag volume fraction of about 20%, where current percolation through Ag channels begins, the composite resistivity is solely dictated by the intragranular resistivity of YBCO corresponding to the resistivity of single crystals and epitaxial thin films. We show that granularity control with varying Ag vol.% in the composites all prepared under an identical sintering scheduled is equivalent to the granularity control in Ag free YBCO prepared by varying the sintering schedule. Based on the variation of the granularity

parameters with Ag vol.%, a grain growth mechanism leading to larger grains with narrower size distribution in the composites is proposed.

Refeences

1. D. Pavuna, H. Berger, M. Affronte, J. Van der Maans, J.J. Capponi, M. Guillot, P. Lejay, J.L. Tholence, Solid State Comm. **68** (1988) 535.
2. B. Dwir, M. Affronte and D. Pavuna, Appl. Phys. Lett. **55** (1989) 399.
3. A. Goyal, S.J. Barns and P.D. Funkenbusch, Phycica C **168** (1990) 405.
4. J. Halbritter, International Journal of Modern Phys. B **3** (1989) 710.
5. J.A. Veira and F. Vidal, Physica C **159** (1989) 468.
6. A. Diaz, J. Maza and F. Vidal, Phys. Rev. B **55** (1997)1209 .
7. J. Maza, F. Vidal, Phys. Rev. B **43** (1991) 10560.
8. A. Diaz, A. Pomar, G. Domarco, J. Maza and F. Vidal, J. Appl. Phys. **77** (1995) 765.
9. J. Lin and Teng-Ming Chen, Z. Phys B-Cond. Matter **81** (1990) 13.
10. J. Halbritter, M.R. Dietrich, H. Kupfer, B. Runtsch, and H.Z. Wiihl, Z. Phys. B-Conden. Matter **71** (1988) 411.
11. A. Diaz, A. Pomer, G. Domarco, J. Maza, J. and F. Vidal, Appl. Phys. Lett. **63** (1993) 1684.
12. J.M. Ziman, : Electrons and Phonons, Oxford : Clarendon Press 1960.
13. A. Kapitulnik, Physica C **153-155** (1988) 520.
14. H.L. Stormer, A.F. Levi, K.W. Baldwin, G.S. Boebinger, Phys. Rev. B **38** (1988) 2472.
15. F.C. Fonseca, R. Muccillo, Physica C **267** (1996) 87.
16. P. Rodrigues, L. Ghivelder, P. Pureur, and S. Reich, Physica C **211** (1993) 13.
17. D. Kumar, P.R. Apte, R. Pinto, S.P. Pai, S.C. Purandre and R. Vijay Raghavan, Journal of Superconductivity **9** (1996) 1.

18. J. Jung, M.A.K. Mahamed , S.C. Cheng and J.P. Frank, Phys. Rev. B **42** (1990) 6181.

19. B. Ropers, R. Canet, F. Carmona and S. Flandrois, Solid State Comm. **75** (1990) 791.

20. U. De, S. Natarajan, and E.W. Seibt, Physica C **183** (1991) 83.

21. B. Batlogg, in Physics of High Temperature Superconductors, S. Mackawa and M. Sato, eds.(Springer-Verlag. Berlin, 1992) P. 219

22. A. Bailey, G. Alvarez, T. Puzzer, K. Sealy, G.J. Russel and K.N.R. Taylor, Mineral Sci. Eng. B **8** (1991) 161.

23. C. Varanasi, M. Hauck, P.J. McGinn, Supercond. Sci. Technol **8** (1995) 879.

24. F. Deslandes, B. Raveau, P. Dobots, D. Legat, Solid State Comm. **71** (1989) 407.

25. J.M. Ting, and R.Y. Lin, Journal of Material Sci. **29** (1994) 1867.

26. D.L. Johnson, J. Am. Ceramic Soc. **53** (1970) 574.

27. M.V. Jacob, J. Mazierska, J. Kim, K.Y. Kang and G.P. Srivastava, Supercond. Sci. Technol. **11** (1998) 1217.

28. D. Kumar, P.R. Apte and R. Pinto, J. Appl. Phys. **77** (1995) 5802.

29. C. Rath, K.K. Sahu, N.C. Mishra, R.P. Das and K. Patnaik, Materials Science Forum **223-224** (1996) 287.